TR-1221

ANALYSIS OF THE SPIRAL ANTENNA DIRECTION FINDER

Peter B. Johnson

20 April 1964

HARRY DIAMOND LABORATORIES
FORMERLY: DIAMOND ORDNANCE FUZE LABORATORIES
ARMY MATERIEL COMMAND
WASHINGTON 25, D. C.

HARRY DIAMOND LABORATORIES

Milton B. Hochmuth
Lt. Col., Ord Corps
Commanding

B. M. Horton
Technical Director

MISSION

(1) Perform basic and applied research in (but not restricted to) the fields of radiating or influence fuzing, time fuzing (electrical, electronic, delay, or fluid), and selected command fuzing for target detection, signature analysis, and the target intercept phase of terminal guidance.

(2) Perform weapon systems synthesis and analysis to determine characteristics that will affect fuze design to achieve optimum weapon effects.

(3) Perform basic and applied research, in support of the functions in (1) above, designed to achieve maximum immunity to adverse influences, including countercountermeasures, nuclear environment, battlefield conditions, and high altitude and space environment.

(4) Perform basic and applied research, in support of assigned missions, or as directed by the Director of Research and Development, AMC, on instrumentation, measurement, and simulation; on materials, components, and subsystems, including electronic timers for weapons; and on selected advanced energy transformation and control systems.

(5) Conduct basic research in the physical sciences, as directed by the Director of Research and Development, AMC.

(6) Perform basic and applied research on fluid amplification and control and development of pure fluid devices and systems.

(7) In support of other AMC elements having project management or commodity management responsibility for specific systems or items, or as assigned by the Director of Research and Development, AMC, perform development (including industrial and maintenance engineering and related prototype production) of:

(a) Proximity fuzes, radiating or influence field.
(b) Time fuzes, electrical, electronic, delay, or fluid.
(c) Selected command fuzes.

UNITED STATES ARMY MATERIEL COMMAND
HARRY DIAMOND LABORATORIES
WASHINGTON 25, D.C.

DA1P222901A207
AMCMS5221.11.17500
HDL Proj. #26100

TR-1221

20 April 1964

ANALYSIS OF THE SPIRAL ANTENNA DIRECTION FINDER

Peter B. Johnson

FOR THE COMMANDER:
Approved by

H. Sommer
Chief, Laboratory 200

Page 2 Blank

CONTENTS

Page 4 Blank

ABSTRACT

A study was made of a method previously suggested for constructing a passive direction finder capable of determining the azimuth and elevation of an electromagnetic wavefront. This direction finder consists of a two-wire, Archimedian, spiral antenna and a phase comparator. Angular information of accuracy too low for the intended application is obtained when the theory and experimental data previously presented are used. A general theory for the direction finder is established and methods for accuracy improvement are suggested.

1. INTRODUCTION

Kaiser et al proposed a spiral antenna direction finder described in reference 1. It was assumed that two radiation modes are characteristic of the Archimedian spiral antenna (of appropriate diameter) and that the potentials at the points C and C' in figure 1 due to a wavefront arriving with coordinates θ (elevation angle) and φ (azimuthal angle) may be represented by equations (1) and (2).

$$\text{Potential on line C} = E_{\text{mode 2}} = Ae^{j2\varphi} \sin\theta\, e^{j\omega t} \qquad (1)$$

$$\text{Potential on line C'} = E_{\text{mode 1}} = Be^{j\varphi} \cos\theta\, e^{j\omega t} \qquad (2)$$

In the present study it was found that the use of equations (1) and (2) in conjunction with the experimental data previously presented (ref 2) leads to errors in the determination of θ and φ. Experimental values of $\sqrt{P_a}$ and $\sqrt{P_b}$ are compared in figures 2 and 3 with the theoretically predicted values from equations (1) and (2). P_a and P_b are the detected values of the signals due to the first and second modes, respectively.

If the crossover point of the radiation patterns of the two modes is unique and occurs at θ_o, then

$$A \sin\theta_o = B \cos\theta_o$$

and it can be shown that

$$\theta = \tan^{-1}\{\tan\theta_o \sqrt{P_a/P_b}\}$$

The quantities $\tan\theta$ and $\tan^{-1}[\tan\theta_o \sqrt{P_a/P_b}]$ are compared in figure 4.

Errors also occur when the experimental data are used to compute φ. A table comparing some experimentally determined values of φ with true values of φ is given in appendix A. The comparisons are made at

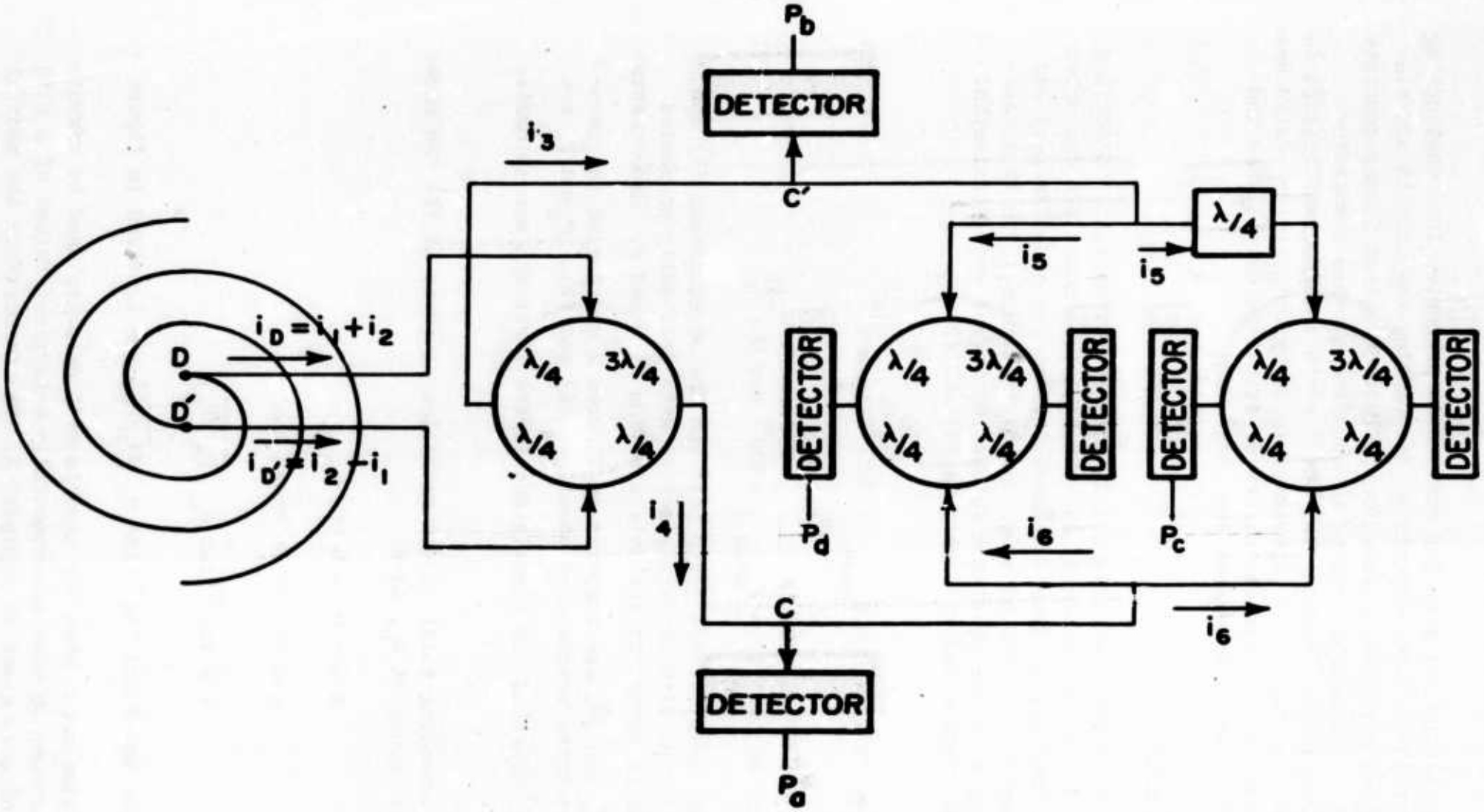

Figure 1. Schematic for the spiral antenna direction finder.

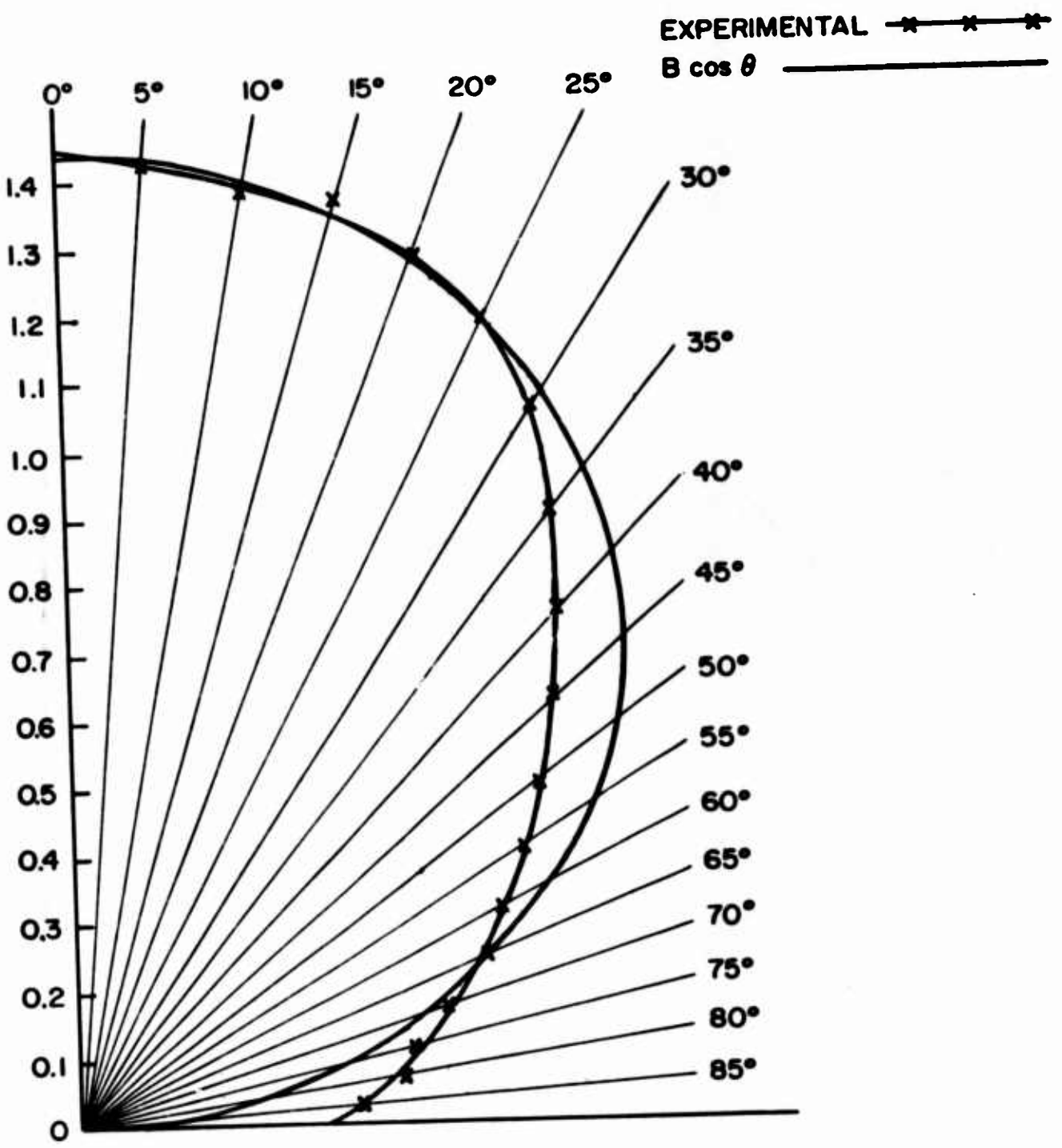

Figure 2. A comparison of the first mode radiation pattern with B cos θ as a function of θ.

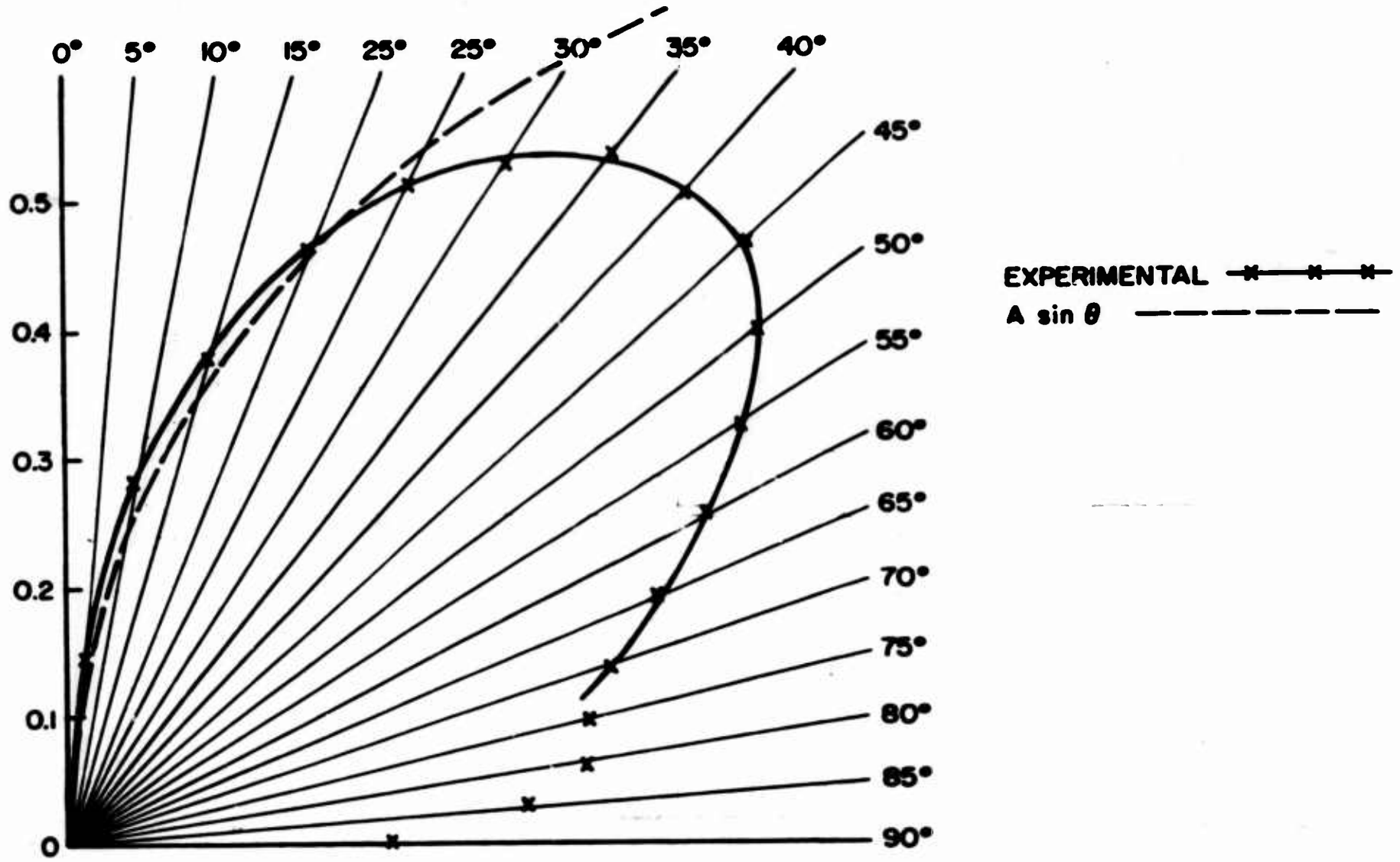

Figure 3. A comparison of the second mode radiation pattern with A sin θ as a function of θ.

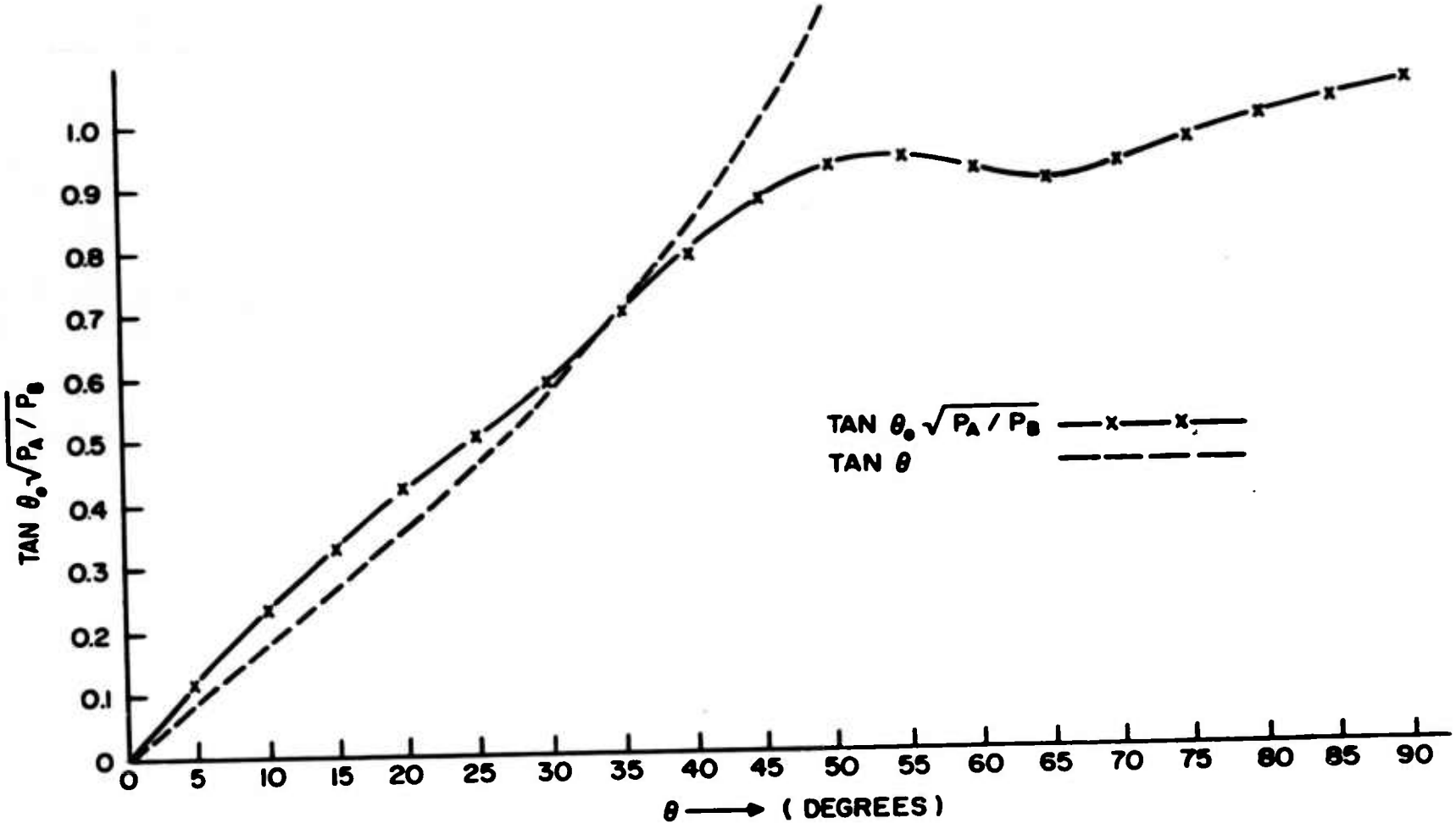

Figure 4. A comparison of tan θ with tan $\theta_o \sqrt{P_A/P_B}$.

intervals of 15°. The table is intended to be indicative of errors in φ and not a comprehensive measure of the error. The largest single discrepancy so found between the true value and measured value of φ is 14.1°. The root-mean-square error for φ for the set of points tabulated in appendix A is 5.8°.

We are interested in improving the accuracy of the direction finder. For the purpose intended it was desired to achieve an accuracy of 0.5 deg.

This report consists of six sections: (1) Introduction, (2) General Theory of Direction-Finder Operation, (3) Mathematical Pattern Representation, (4) Changes in Antenna Structure to Obtain Pattern Fit, (5) Error Analysis, and (6) Conclusions.

Section 2 establishes a general theory for direction-finder operation. This theory uses Kaiser's ideas as a base and adds theoretical knowledge of the equiangular spiral antenna to aid in a more general formulation of the direction-finding problem. (Given amplitude and phase information from two antennas, we seek to establish that it is possible by appropriate manipulation to determine the azimuth and elevation of a source.) It is later suggested that the Archimedian antenna can be considered to be a special case of the equiangular antenna. The general formulation of section 2 describes a need for establishing a mathematical representation for the ratio of antenna amplitude patterns. This ratio is a function of the elevation angle, θ. Two methods for obtaining this representation are suggested. Section 3 describes the first method, a technique for fitting an experimentally obtained ratio with a set of decaying exponentials. The technique is demonstrated (as an example) by fitting the data given by Kaiser for his Archimedian antenna. Section 4 describes an alternate method for obtaining a mathematical representation of the desired ratio. First, a theoretical description of the antenna radiation patterns is presented. (This theory is also required in section 2 to aid in establishing the general theory.) By the manipulation of a critical antenna design parameter, the radiation patterns of the antenna can be theoretically manipulated so that the desired ratio closely approximates a known function. Again, the technique is demonstrated as an example. The errors that are incurred by the use of the Archimedian antenna (as experimentally presented by Kaiser) are examined in section 5 with the aid of the general theory.

2. GENERAL THEORY OF DIRECTION FINDER OPERATION

To understand the theoretical operation of the direction finder, it is necessary to consider some of the characteristics of the spiral antenna. We assume that the antenna can operate in only two basic modes. We will say the first mode has been excited when currents that are out of phase are generated by the antenna on lines D and D' (fig. 1) [line D with $i_1 e^{j\omega t}$ and line D' with $i_1 e^{j(\omega t + \pi)}$]. Similarly, we will say that the second mode has been excited when lines D and D' carry currents that are in phase [lines D and D' with $i_2 e^{j\omega t}$].

We assume that the currents on lines D and D' due to simultaneous reception of the first and second modes have an amplitude and phase structure that is a linear combination (superposition) of the amplitudes and phase structures of the currents due to the first and second modes. Then, in general, line D will carry a current $i_1 e^{j\omega t} + i_2 e^{j\omega t}$ and line D' will carry a current $i_1 e^{j(\omega t + \pi)} + i_2 e^{j\omega t}$.

We assume the following general representations for i_1 and i_2.

$$i_1(t,\theta,\varphi) = f_1(\theta,\varphi) e^{jP_1(\theta,\varphi)} e^{j\omega t}$$

$$i_2(t,\theta,\varphi) = f_2(\theta,\varphi) e^{jP_2(\theta,\varphi)} e^{j\omega t}$$

Therefore,

$$i_D(t,\theta,\varphi) = [f_1 e^{jP_1} + f_2 \, {}^{jP_2}] \, e^{j\omega t}$$

Similarly,

$$i_{D'}(t,\theta,\varphi) = [f_1 e^{j(P_1+\pi)} + f_2 e^{jP_2}] \, e^{j\omega t}$$

When the signals i_D and $i_{D'}$, are processed by the first phase comparator (thus performing an addition and a subtraction) the result is:

a. On line C (the line where the sum, $i_D + i_{D'}$, appears)

$$i_3(t,\theta,\varphi) = 2f_2 e^{jP_2} \, e^{j\omega t}$$

b. On line C' (the line on which the difference, $i_D - i_{D'}$, appears)

$$i_4(t,\theta,\varphi) = 2f_1 e^{jP_1} \, e^{j\omega t}$$

If half the power of the signal in each line is detected (square law) P_a and P_b are generated.

$$P_a = 2f_1^2 \quad (\theta, \varphi) \tag{3}$$

$$P_b = 2f_2^2 \quad (\theta, \varphi) \tag{4}$$

If i_5 is delayed by 90° and added to i_6 (as shown in fig. 1) and then detected, P_c results.

$$P_c = \{f_1^2 + f_2^2 + 2f_1f_2 \sin (P_2 - P_1)\} \tag{5}$$

If i_6 is added to i_5 and then detected, P_d results.

$$P_d = \{f_1^2 + f_2^2 + 2f_1f_2 \cos (P_2 - P_1)\} \tag{6}$$

These are the only quantities essential for the direction finder operation.

We wish to show that θ and φ can be found by solving equations (7), (8), and (9), simultaneously.

$$(f_1/f_2)^2 = P_a/P_b \tag{7}$$

$$P_2 - P_1 = \sin^{-1}\left[\frac{P_c - f_1^2 - f_2^2}{2 f_1 f_2}\right] = \sin^{-1}\left[\frac{2 P_c - P_a - P_b}{2(P_a P_b)^{\frac{1}{2}}}\right] \tag{8}$$

$$P_2 - P_1 = \cos^{-1}\left[\frac{P_d - f_1^2 - f_2^2}{2 f_1 f_2}\right] = \cos^{-1}\left[\frac{2 P_d - P_a - P_b}{2(P_a P_b)^{\frac{1}{2}}}\right] \tag{9}$$

Equation (7) is the result of taking the ratio of equations (3) and (4). The ratio $(f_1/f_2)^2$ is known from experiment to be a strong function of θ and a weak function of φ. Equations (8) and (9) are the result of solving equations (5) and (6) for $P_2 - P_1$. The difference $P_2 - P_1$ is known to be a strong function of φ and a weak function of θ. Both equations (8) and (9) are needed to determine the quadrant of φ unamibiguously.

Conditions must be attached to f_1, f_2, P_1, and P_2, to guarantee a solution and to establish that θ and φ can be unambiguously determined. We have written these functions in as general a form as possible so as to allow for the incorporation of the greatest latitude in the behavior of the antenna.

To make simplifying assumptions about f_1, f_2 P_1, and P_2, we need

to anticipate material that appears in section 4, where it is established that the far radiation field of the spiral antenna for a specific mode may be represented as the product of a function of θ and a function of φ of the form

$$E_n = \mathcal{K}_n(\theta)e^{jn\varphi}e^{j\omega t}$$

where n refers to the mode number. For the first mode n = 1. Furthermore (from section 4):

$$\mathcal{K}_n(\theta) = F_n(\theta)e^{-jR_n(\theta)}$$

Substituting for $\mathcal{K}_n(\theta)$

$$E_n = F_n(\theta)e^{-jR_n(\theta)}e^{jn\varphi}e^{j\omega t} = F_n(\theta)e^{j[n\varphi - R_n(\theta)]}e^{j\omega t}$$

We now identify $F_n(\theta)$ as $2f_n(\theta)$ (f_1 and f_2 as defined on page 11)

and $P_n(\theta,\varphi)$ as $[n\varphi - R_n(\theta)]$ (P_1 and P_2 as defined on page 11).

$$2f_1(\theta,\varphi) = F_1(\theta)$$

$$2f_2(\theta,\varphi) = F_2(\theta)$$

$$P_1(\theta,\varphi) = \varphi - R_1(\theta)$$

$$P_2(\theta,\varphi) = 2\varphi - R_2(\theta)$$

Therefore

$$f_1/f_2 = F_1/F_2$$

$$P_2 - P_1 = \varphi - R_1 + R_2$$

It follows that

$$P_a/P_b = (F_1/F_2)^2 \qquad (10)$$

$$\varphi = \cos^{-1}\left[\frac{2P_c - P_a - P_b}{2(P_aP_b)^{\frac{1}{2}}}\right] - R_1(\theta) + R_2(\theta) \qquad (11)$$

$$\varphi = \sin^{-1}\left[\frac{2P_d - P_a - P_b}{2(P_aP_b)^{\frac{1}{2}}}\right] - R_1(\theta) + R_2(\theta) \qquad (12)$$

In order that the direction finder be unambiguous in a hemisphere [$0^\circ \leq \varphi \leq 360^\circ$, $0^\circ \leq \theta \leq 90^\circ$], it is necessary to place restrictions on the ratio F_1/F_2 and the difference $P_2 - P_1$. It is sufficient to require that the ratio F_1/F_2 be monotonic on $0^\circ \leq \theta \leq 90^\circ$ (or a subinterval of interest) and that F_1, $F_2 > 0$. To assure uniqueness of $P_2 - P_1$, it is sufficient to require that the difference $R_1 - R_2$ be single valued for all θ. Equations (7), (8) and (9) have been written in terms of ratios of the detected quantities. This is necessary to eliminate the effects of gain.

3. MATHEMATICAL PATTERN REPRESENTATION

We wish to find a function to approximate experimentally measured direction-finder data. We desire an expression for the ratio $(F_1/F)^2$ from equation (10).

This is done as an example for the ratio computed from experimental data taken by Kaiser (ref 2). This ratio is shown in figure 5.

Note that the experimental curve, $\mathfrak{J}(\theta)$, is monotonic only on the restricted interval $0^\circ \leq \theta \leq 60^\circ$ and not for $0^\circ \leq \theta \leq 90^\circ$, as is necessary to give hemispheric direction finding. This means the direction finder will give an unambiguous output only on the restricted interval. Nothing can be done to extend the useful range of θ for this example since this restriction is assumed to be a characteristic of the Archimedian spiral antenna. We desire to approximate the experimental curve $\mathfrak{J}(\theta)$, with high accuracy and by a simple approximation function. In general this is best accomplished by choosing an approximating function similar in nature to the signal to be represented. In this case, the signal to be represented appears to be similar to a decaying exponential, and therefore an attempt will be made to represent it as a combination of decaying exponentials. As a first approximation, $\mathfrak{J}(\theta)$ is to be represented on the interval $5^\circ \leq \theta \leq 60^\circ$ as

$$\mathfrak{J}(\theta) \approx g(\alpha) = \beta_1 e^{k_1\alpha} + \beta_2 e^{k_2\alpha} + \beta_3 e^{k_3\alpha}$$

where $\alpha = \theta - 5^\circ$. The redefinition of θ is not essential but is helpful to avoid difficulties at the origin. These difficulties occur because P_b becomes small causing the ratio P_a/P_b to become large. We choose $k_3 = -0.03\ (\text{deg})^{-1}$ because it "fits" $\mathfrak{J}(\alpha)$ in the region $40^\circ \leq \alpha \leq 55^\circ$ and therefore approximates the "slow" (slowly changing)

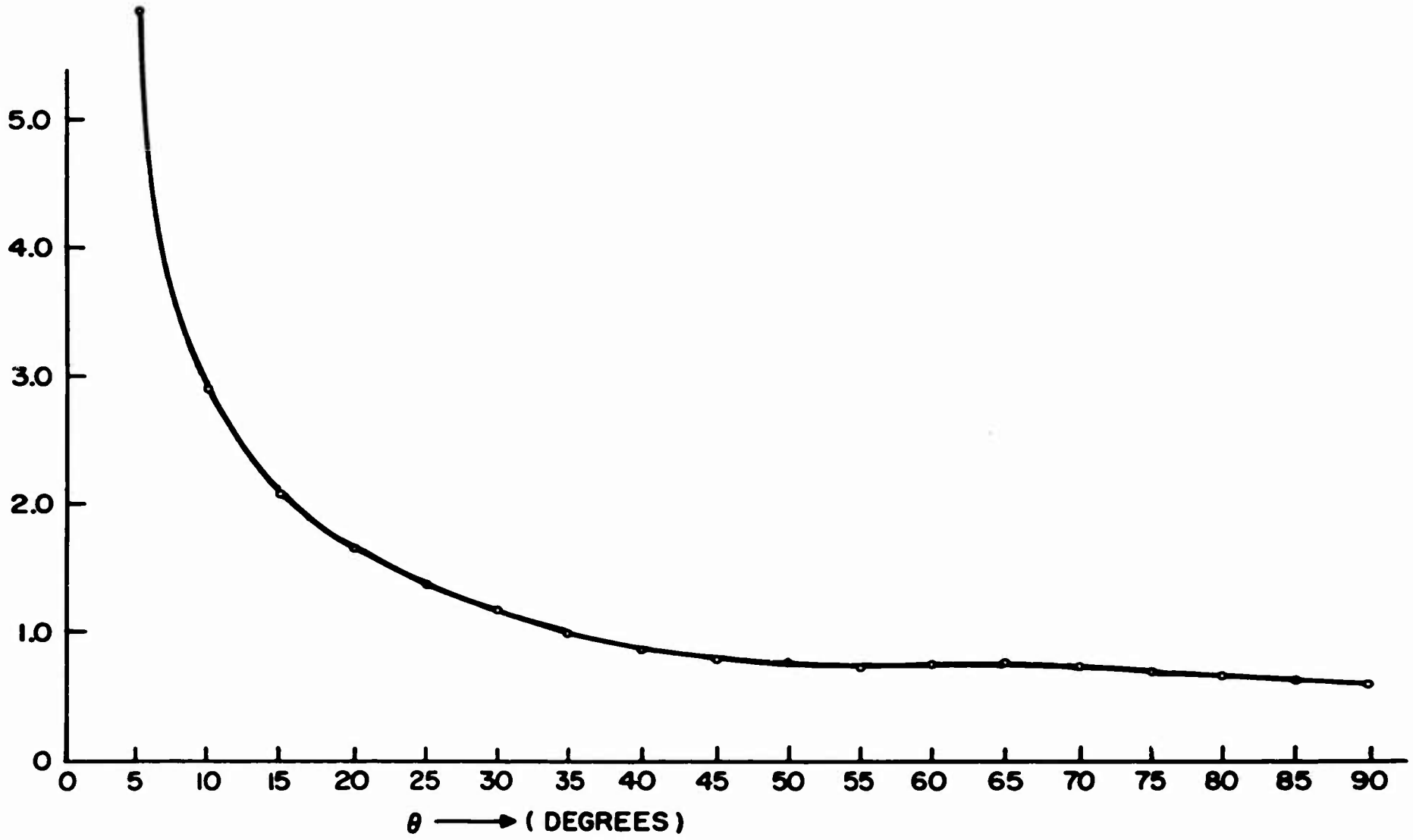

Figure 5. P_a/P_b as a function of θ. Points computed from experimental data at 5^o intervals $P_a/P_b = J(\theta)$.

part of the curve. We choose $k_1 = -0.10\ (\text{deg})^{-1}$ because it "fits" $\mathfrak{G}(\alpha)$ for $0^o \leq \alpha \leq 10^o$ and therefore approximates the "fast" (quickly changing) part of the curve. We choose $k_2 = -0.065\ (\text{deg})^{-1}$ because it is between the slow and the fast constants. These basis functions are truncated at $\alpha = 55^o$.

It would be desirable to choose the k's so that

$$\left.\begin{array}{l} |\mathfrak{G}(\alpha) - g(\alpha)| < \epsilon_1 \\ \text{or} \\ [\mathfrak{G}(\alpha) - g(\alpha)]^2 < \epsilon_2 \end{array}\right\} \text{for } 0^o \leq \alpha \leq 55^o$$

where ϵ_1 or ϵ_2 is to be as small as possible. Unfortunately these k's cannot be found easily because the equations that result from a least square or absolute value optimization technique are nonlinear and have not been solved analytically as far as is known. It is believed that high-speed digital computing techniques could be employed to find the best k's. However, if values of k_i are assumed, the β's can be chosen so that $g(\alpha)$ approximates $\mathfrak{G}(\alpha)$ in the least square sense with respect to the β's. When this is done the following equation is obtained:

$$g(\alpha) = 13.2e^{-0.1\alpha} - 13.4e^{-0.065\alpha} + 5.6e^{-0.03\alpha}$$

The details of this calculation are given in appendix B. $g(\alpha)$ can be made to approximate $\mathfrak{G}(\alpha)$ as closely as desired by using a greater number of basis functions. A comparison of $\mathfrak{G}(\alpha)$ and $g(\alpha)$ is made in figure 6.

4. CHANGES IN ANTENNA STRUCTURE TO OBTAIN PATTERN FIT

As an alternate approach, it may be possible to modify the antenna structure so that the first and second radiation modes can be accurately represented by some simple functions.

Changes can be made in the structure in a number of ways, some of which are:

(1) The spacing between the arms of the Archimedian antenna can be changed. This can be accomplished by varying b in the equation that defines the Archimedian antenna, $r = b\,\theta$.

(2) The type of antenna can be changed from Archimedian to equiangular and the c in the equation $r = e^{c\theta}$ can be varied.

(3) A reflecting cavity behind the antenna can be changed in shape and position.

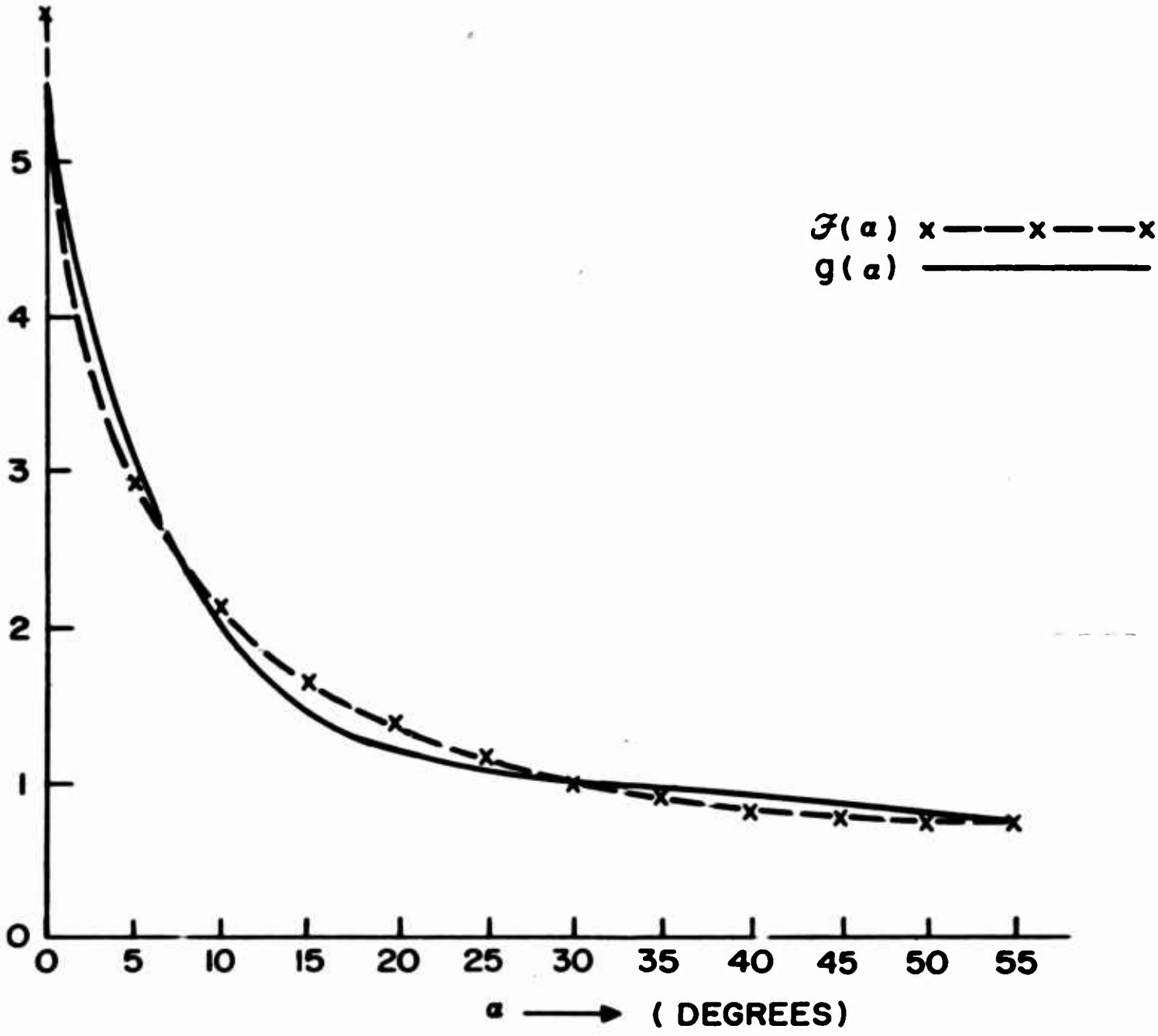

Figure 6. A comparison of $\mathfrak{F}(\alpha)$ and $g(\alpha)$ as functions of α.

(4) The dielectric constant of the material used for mounting the antenna can be varied.

Of these possibilities only the first and second are considered to be basic. By varying b or c the antenna can be changed from a dipole-like structure (b, c = ∞) to an approximately circular structure (0 < b, c < 0.1). If b or c is large (b, c > 0.3), the number of spiral arms must be large (at least greater than two) to maintain a radiation pattern with amplitude independent of φ.

A theoretical analysis of the equiangular antenna sufficient for the purposes of this paper has been made by Cheo (ref 3). His analysis requires the assumption of an antenna that is everywhere conducting in the direction tangent to the curve $r = e^{c\theta}$ and perfectly nonconducting perpendicular to this direction. Furthermore, this antenna is assumed to be center-fed so that the total phase change of the exciting voltage around the center of the antenna is $2\pi n$ radians (n an integer) where n = 1 for the first mode of operation, and n = 2 for the second mode of operation. Cheo assumes the phase change between adjacent feeds to be constant as shown in figure 7. He assumes the number of generators tends to infinity as $\Delta\varphi$ tends to zero. This results in a continuous feeding arrangement.

Cheo theoretically establishes the following results:

$$| E_r | \cong 0, \qquad | E_\theta | = | E_\varphi | \tag{13}$$

where E_r, E_θ, and E_φ are the radial, elevation, and azimuthal components of the electric field, respectively.

$$| E_\theta | = | F_n(\theta) | \, e^{-jR_n(\theta)} e^{jn\varphi} \tag{14}$$

$$| F_n(\theta) | = \frac{\cos\theta \, [\tan(\theta/2)]^n \exp[(n/c)\tan^{-1}(c\cos\theta)]}{\sin\theta \, [1 + c^2\cos^2\theta]^{\frac{1}{2}}} \tag{15}$$

$$R_n(\theta) = (n/2c)\,[\ln(1+c^2)\cos^2\theta] + \tan^{-1}(c\cos\theta) \tag{16}$$

$| F_n(\theta) |$ and $R_n(\theta)$ are plotted for the first and second modes with c as a parameter (n = 1, 2) in figures 8, 9, 10, and 11.

Large changes in shape and amplitude of the radiation pattern occur as c ranges over the values $0.1 \leq c \leq 10$ as may be seen in figures 8 and 9. Negligible changes in the pattern occur for c < 0.1. As

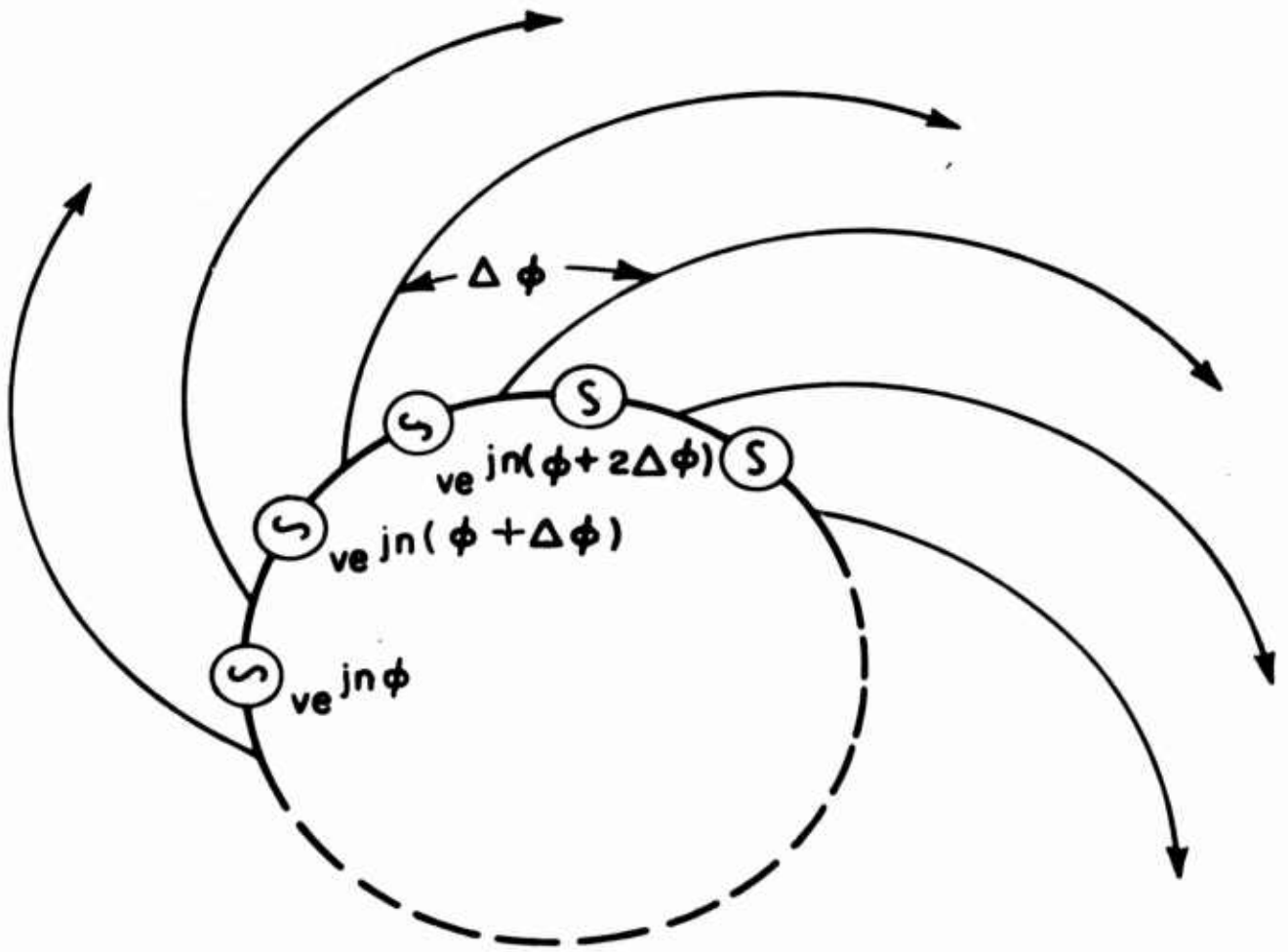

Figure 7. The excitation of the infinitely armed equiangular spiral antenna. n = 1 for the first mode. n = 2 for the second mode.

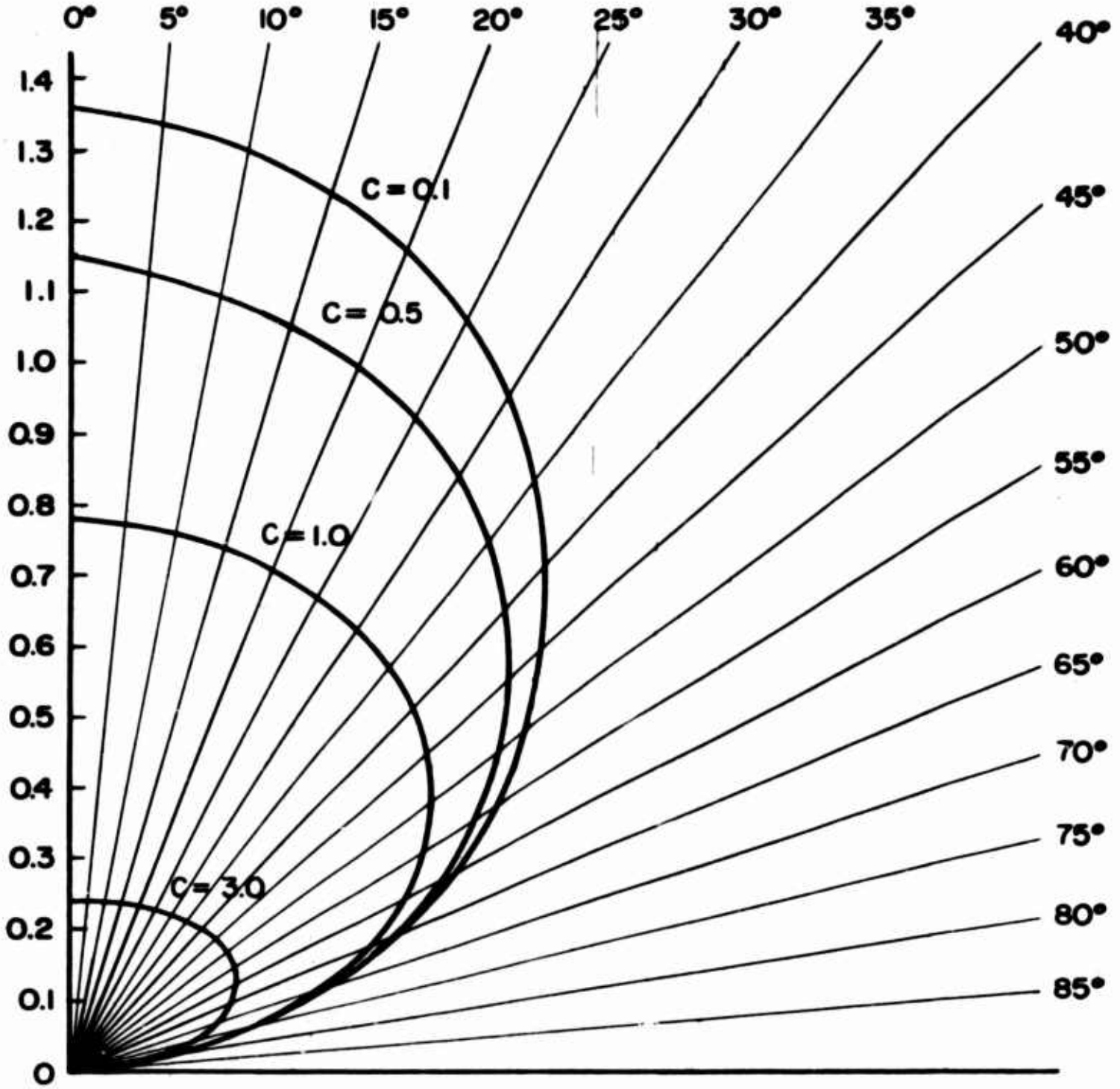

Figure 8. Theoretical first mode radiation pattern, $F_1(\theta)$, for the equiangular spiral antenna as a function of θ.

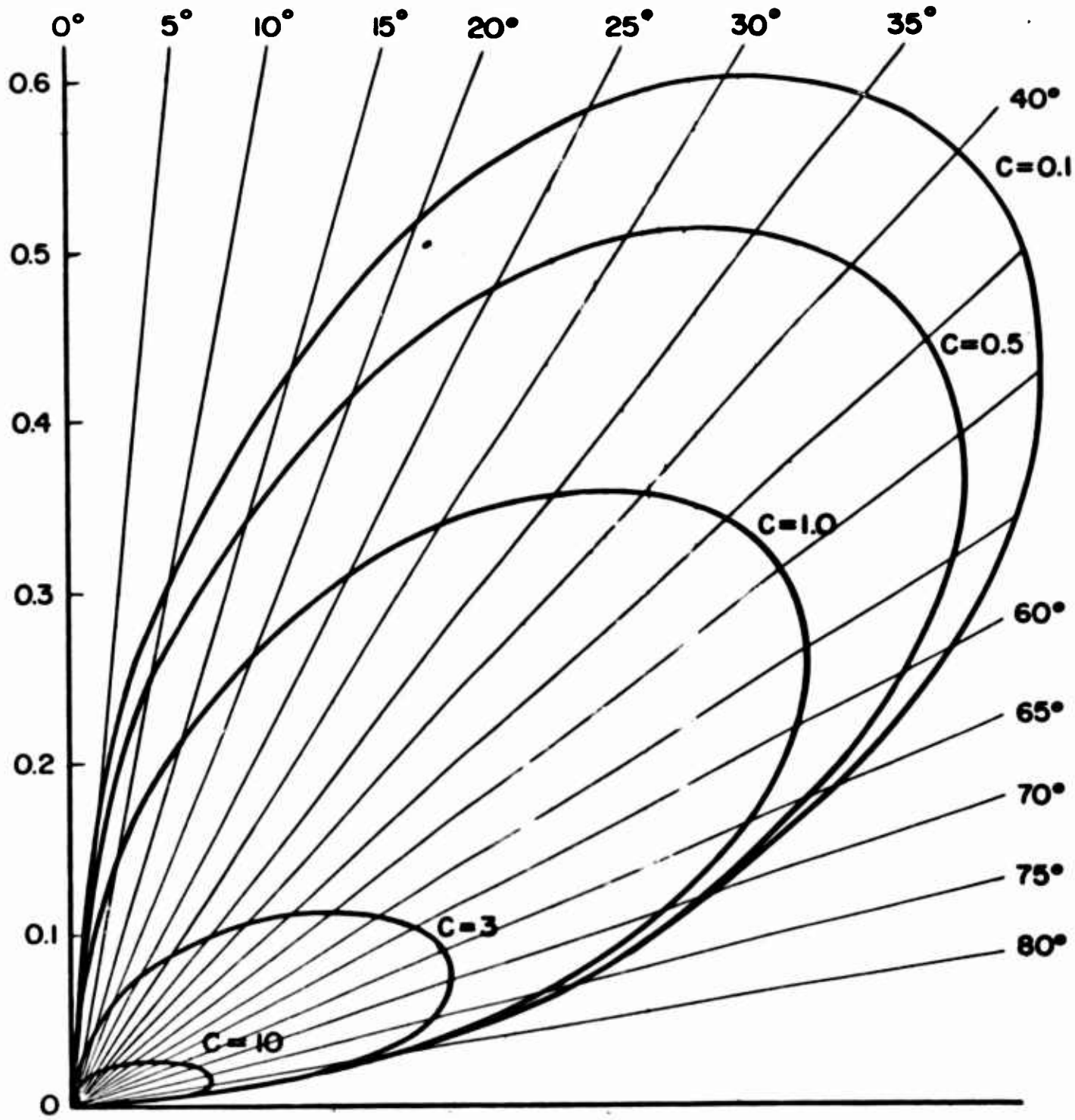

Figure 9. Theoretical second mode radiation pattern, $F_2(\theta)$, for the equiangular spiral antenna as a function of θ.

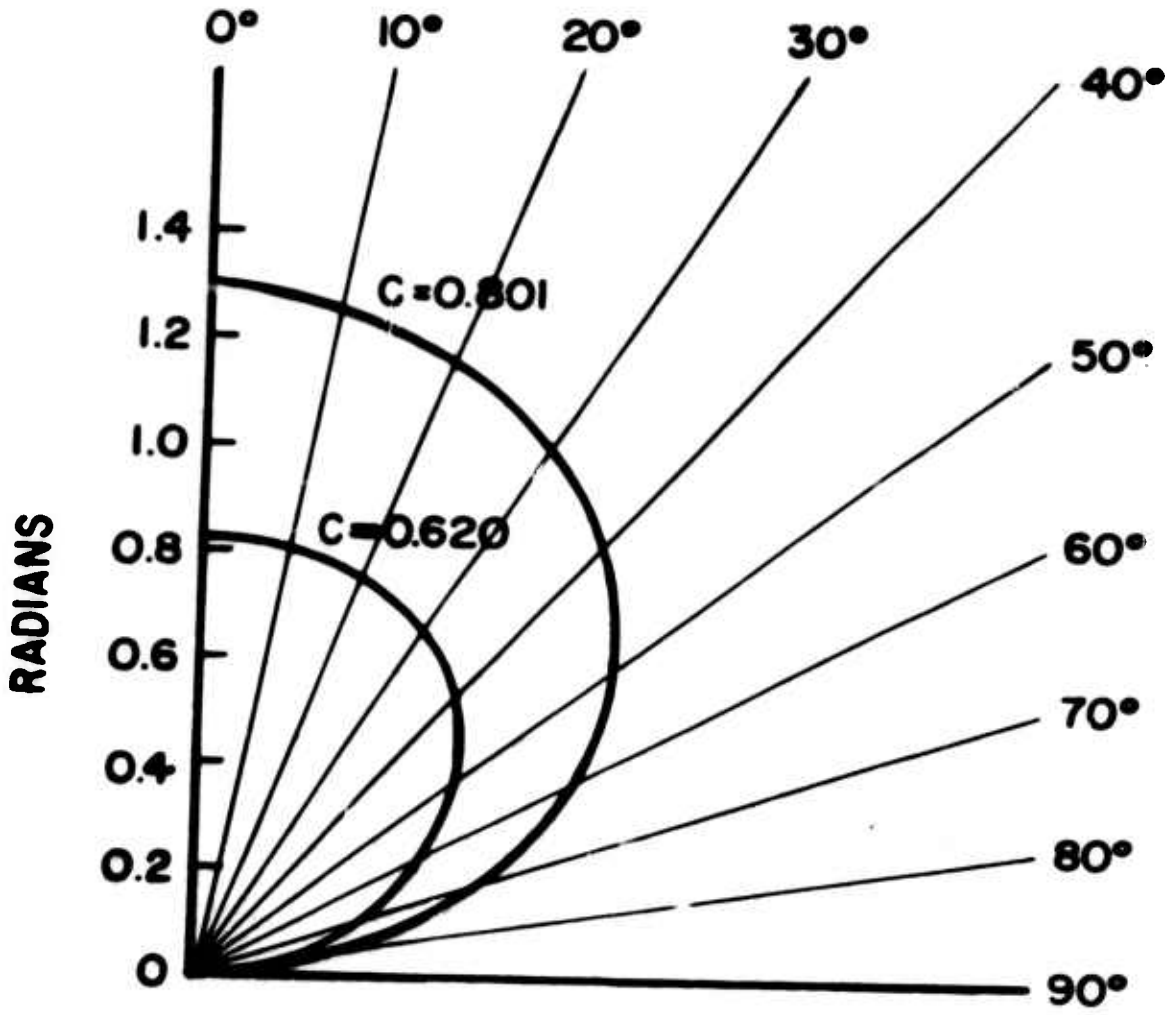

Figure 10. $R_2(\theta)$ as a function of θ with C as a parameter.

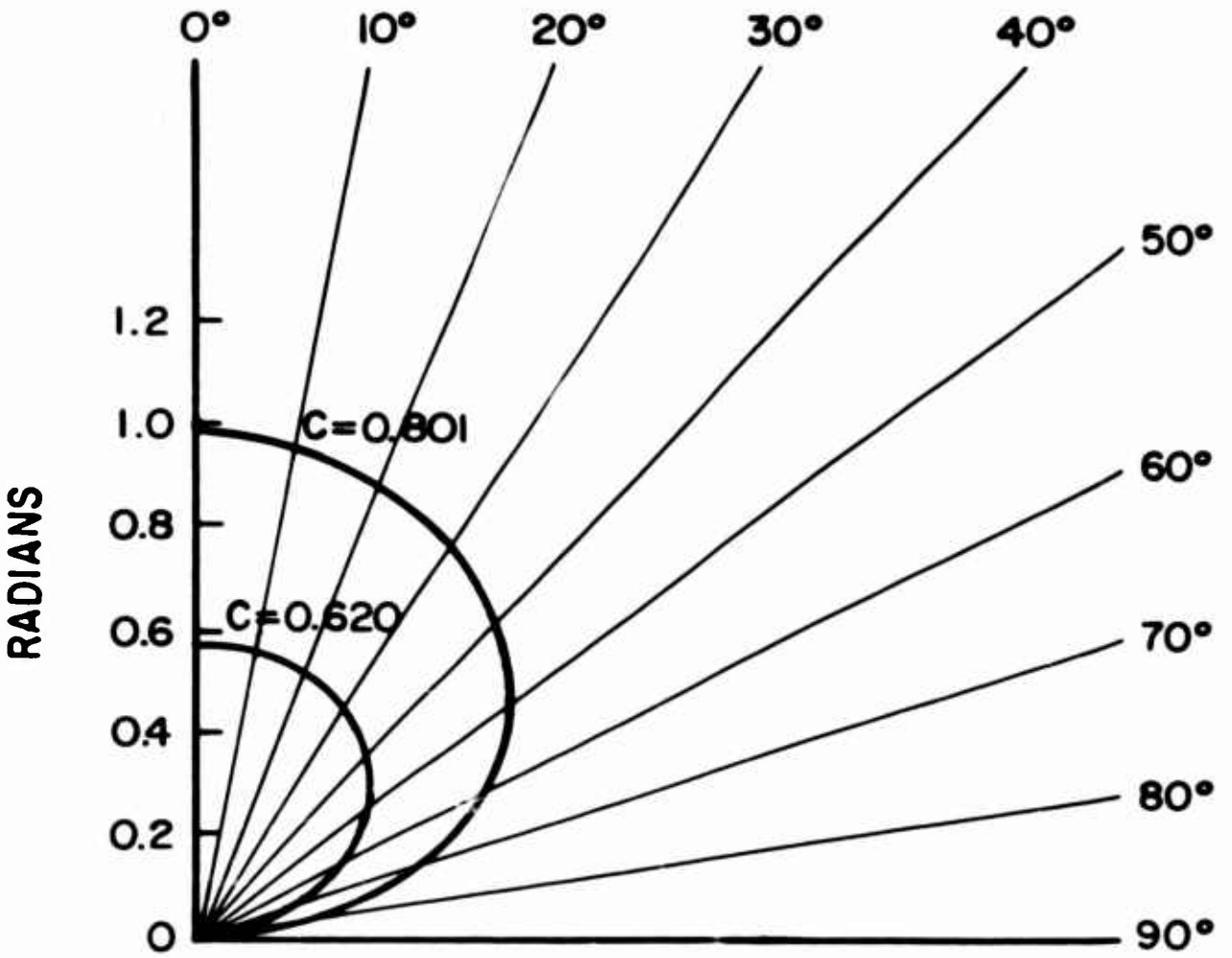

Figure 11. R_1 (θ) as a function of θ with C as a parameter.

mentioned, we wish to adjust c so that the amplitude patterns for the first and second modes are simple functions.

If c is small ($c < 0.1$), the equiangular spiral has the general shape of the Archimedian spiral (b small) for the critical radiating portion of the antenna. If this similarity is accepted, Kaiser's results can be used to confirm Cheo's theoretical findings. Comparison of the experimental and theoretical patterns is made in figures 12 and 13 for $c = 0.05$. Since the value of the gain constant is unimportant, it has been adjusted to give the best agreement for small values of θ.

A digital computer was programed to calculate numerical values of $F_n(\theta)$ at intervals of $\Delta\theta = 5^o$, where c was an easily varied parameter. When the results of the calculation are examined, it appears that the first radiation mode can be accurately approximated by A cos θ if c is chosen somewhere in the range $0.5 < c < 1$. The value of 0.620 for c (obtained by trial and error) results in the smallest error. In this problem, smallest error is difficult to define since a number of factors need be considered. In general, we want $|F_n(\theta) - A \cos \theta|$ to be as small as possible everywhere on the interval, although large errors for θ near 90^o are more acceptable than for θ near 0^o.

Similarly, it is possible to recognize that the second mode can be approximated by B sin 2θ if c is chosen as $c = 0.801$.

Both values of c were chosen by plotting the difference $[F_1(\theta) - A \cos (\theta)]$ or $[F_2(\theta) - B \sin (2\theta)]$ and adjusting A and c or B and c so that the difference appeared to be as small as possible.

Percent theoretical error is plotted in figures 14 and 15 for the values of c chosen. This error is defined in equation (17).

$$\text{Percent theoretical error} = \frac{\left[\left\{ \begin{matrix} A \cos \theta \\ \text{or} \\ B \sin 2\theta \end{matrix} \right\} - F_n(\theta) \right]}{\left\{ \begin{matrix} A \cos \theta \\ \text{or} \\ B \sin 2\theta \end{matrix} \right\}} 100\% \qquad (17)$$

Unfortunately, since the best value of c for the first mode is different from the best value of c for the second mode, it will be necessary to use two antennas, one on which only the first mode is excited and one on which only the second mode is excited.

We have assumed we can build the antenna so that

$$F_1 = A \cos \theta \qquad (18)$$

$$F_2 = B \sin 2\theta \qquad (19)$$

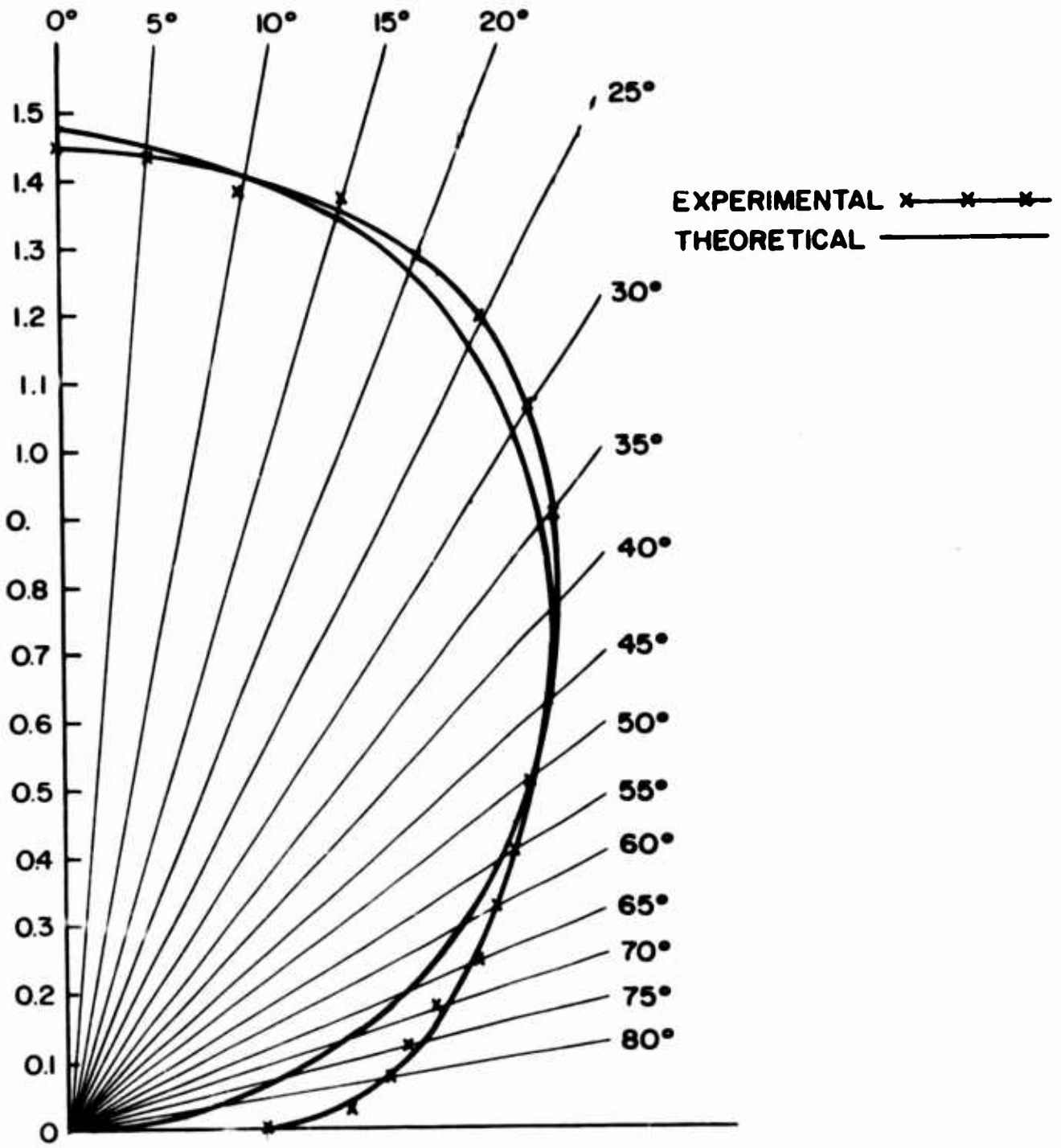

Figure 12. A comparison of theoretical and experimental first mode radiation patterns. C = 0.05

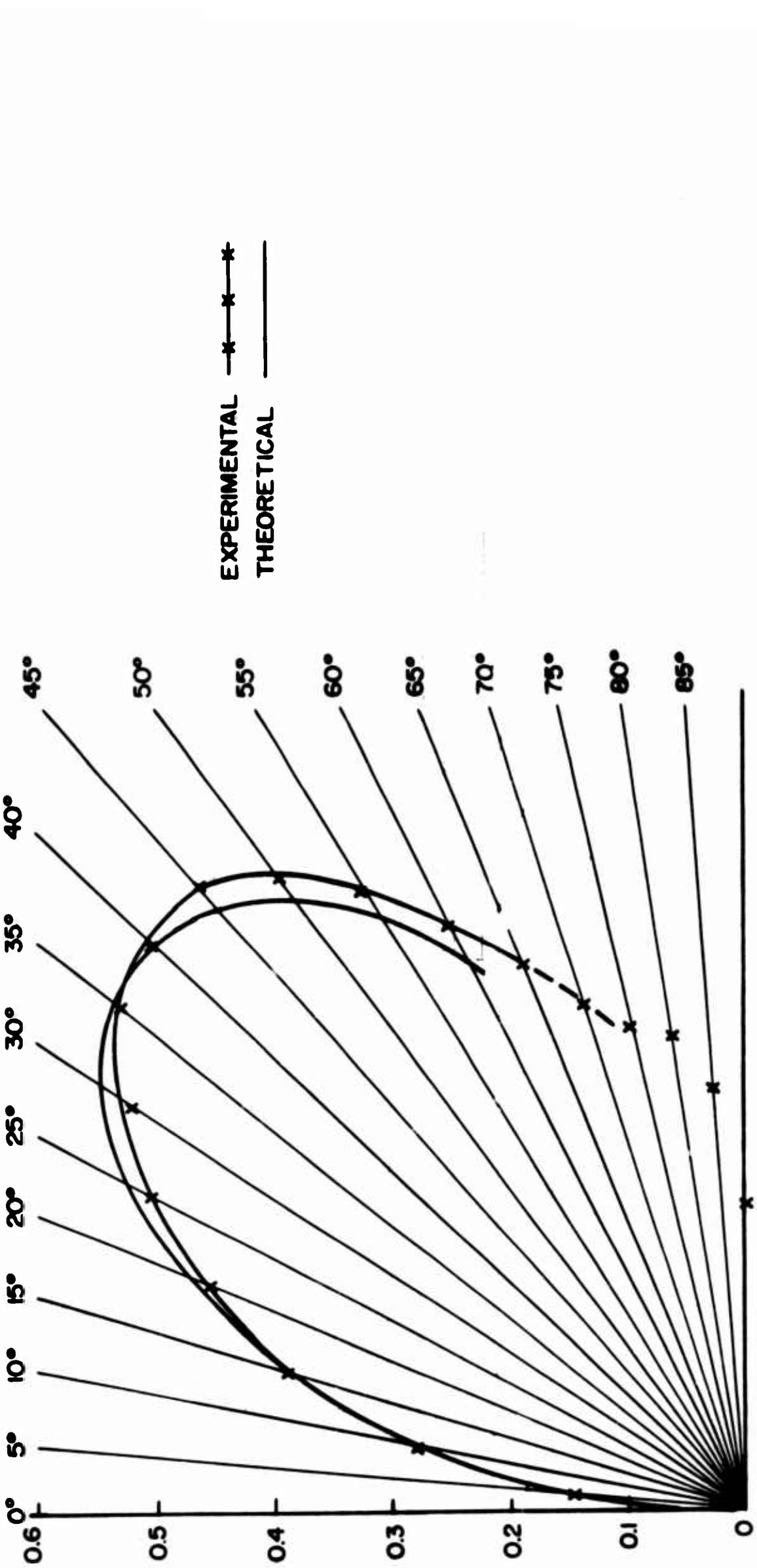

Figure 13. Comparison of theoretical and experimental second mode radiation patterns. C = 0.05.

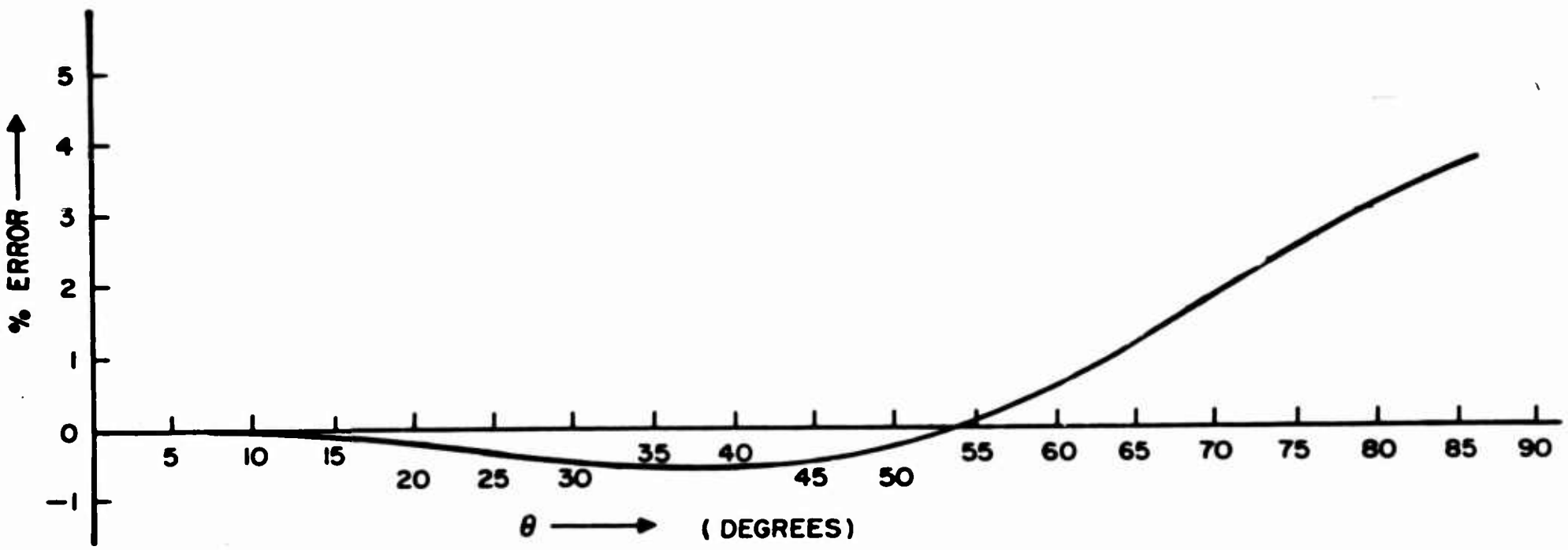

Figure 14. Theoretical error for first mode radiation pattern as a function of θ.
C = 0.620

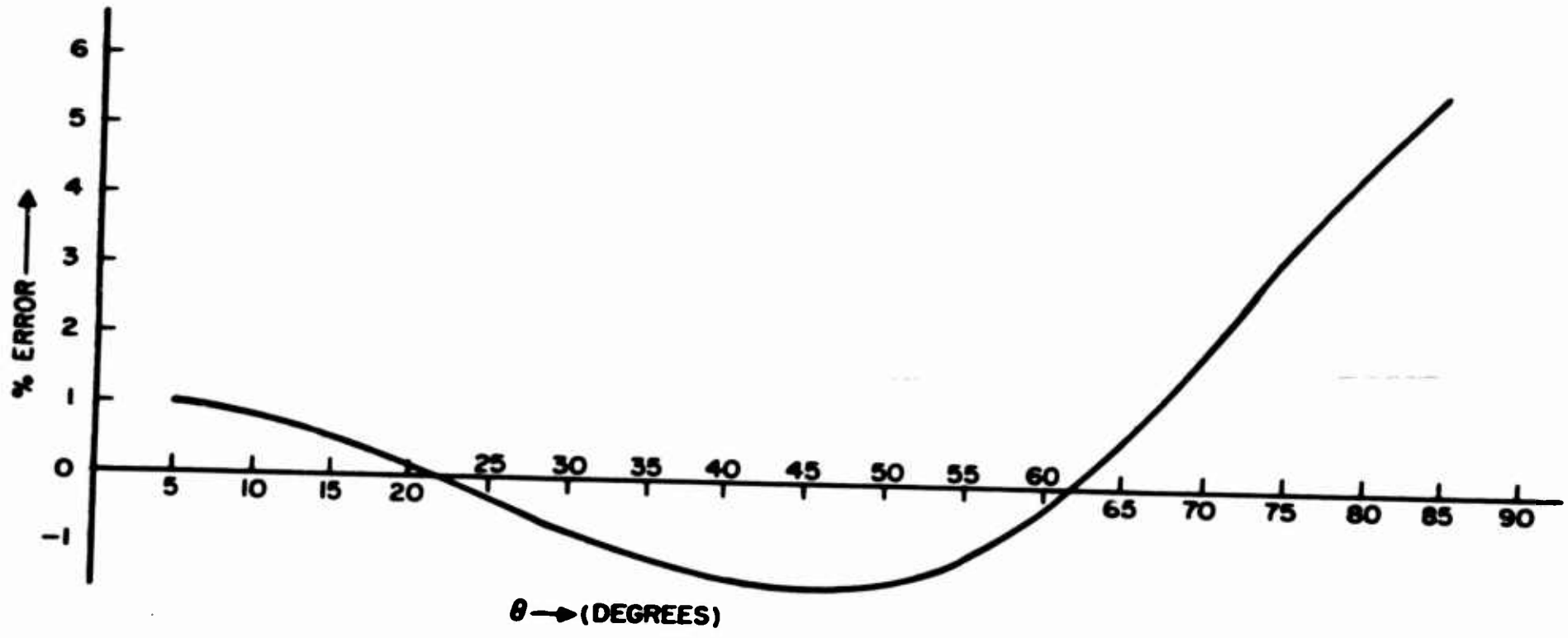

Figure 15. Theoretical error for second mode radiation pattern as a function of θ. C = 0.801.

Recalling the argument presented in section 2, P_1 and P_2 may be written

$$P_1(\theta,\varphi) = \varphi - R_1(\theta) \tag{20}$$

$$P_2(\theta,\varphi) = 2\varphi - R_2(\theta) \tag{21}$$

If the output of the equiangular antenna structure is manipulated by the phase shifter

$$P_a/P_b = \frac{A^2 \cos^2(\theta)}{B^2 \sin^2(2\theta)} = \frac{A^2 \cos^2 \theta}{4B^2 \sin^2(\theta) \cos^2(\theta)}$$

Solving for θ

$$\theta = \sin^{-1}\left\{ \frac{A}{2B} \sqrt{P_b/P_a} \right\}$$

φ can be found from equations (11) and (12) in section 2.

This section suggests a second method for obtaining a mathematical representation for the ratio of antenna amplitude patterns. It also suggests methods for obtaining and manipulating radiation patterns which meet the minimum conditions established in section 2.

5. ERROR ANALYSIS

As mentioned in section 2, the ratio f_1/f_2 must be monotonic for the range of θ of interest. Kaiser's data for the Archimedian antenna are monotonic only for $0^\circ \leq \theta \leq 60^\circ$. This is considered to be a characteristic of the Archimedian spiral antenna and restricts the useful range of θ to be less than 60°. There is also a practical limitation on the useful range of θ due to the f_1/f_2 ratio. Because it is slowly changing from $30^\circ \leq \theta < 60^\circ$, small errors in the computation of the ratio will result in large errors in the determination of θ. This is also considered to be a characteristic of the Archimedian spiral antenna.

The upper and lower bounds on the error made in computing θ when the detected variables are perturbed from their true values are plotted as a function of θ in figure 16. For example, for an input signal perturbation of 1 percent or less, if an actual value of θ is $\theta = 40^\circ$, and if the entire system functions perfectly, the computed value of θ may take on any value in the range $38.2^\circ \leq \theta \leq 44.2^\circ$.

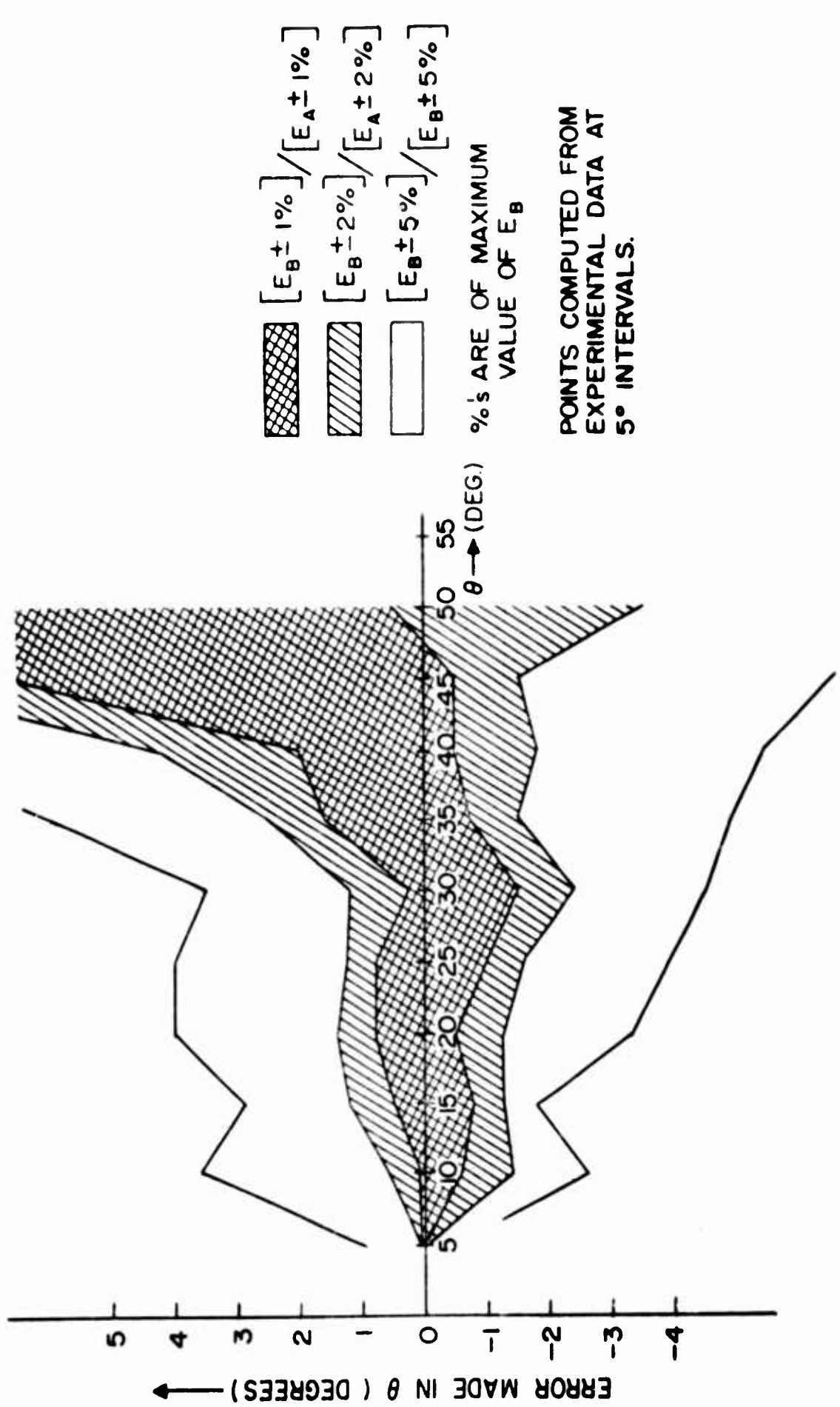

Figure 16. Limits on the error made in computing θ when the detected variables have been perturbed from their true value.

Because f_1/f_2 changes rapidly for small θ, θ can be more accurately determined in this region. Note that because

$$\lim_{\theta \to 0} [f_1/f_2] \qquad \text{becomes large}$$

difficulties may result in determining θ in the range $0^o \leq \theta \leq 5^o$.

Additional errors in the determination of θ will be caused if the ratio is a function of φ (i.e., if pattern asymmetries exist as is the case with the data given by Kaiser). Asymmetries will result in deviations of the ratio from the curve given in figure 5, and errors due to this cause alone can result in errors, ϵ, in the determination of θ of $0^o \leq \epsilon \leq 12^o$. [A comparison of $(f_1/f_2)^2\big|_{\varphi = 0}$ and $(f_1/f_2)^2\big|_{\varphi = 180^o}$ is given in figure 17.]

Errors in the determination of θ resulting from a combination of noise and asymmetries are not additive.

The determination of φ is independent of the amplitude functions, f_1 and f_2. The accuracy of φ depends upon the accuracy of the phase shifting networks in the phase comparator and upon the validity of the assumptions concerning P_1 and P_2.

6. CONCLUSIONS

To determine if the direction finder can or cannot be made to function with greater accuracy, it will be necessary to determine experimentally whether the functions f_1, f_2, R_1, and R_2 can be generated by a spiral antenna to satisfy the conditions previously established. Preliminary information indicates that f_1 and f_2 for the Archimedian antenna are not sufficiently well behaved. No information is available for R_1 and R_2. If the minimum conditions cannot be met by the Archimedian antenna, it may be possible to show that f_1, f_2, R_1, and R_2 can be manipulated so that they satisfy the theoretical requirements by making changes in the antenna design. In summary we need to establish experimentally that we can build an antenna for which:

(1) f_1 and f_2 are independent of φ.

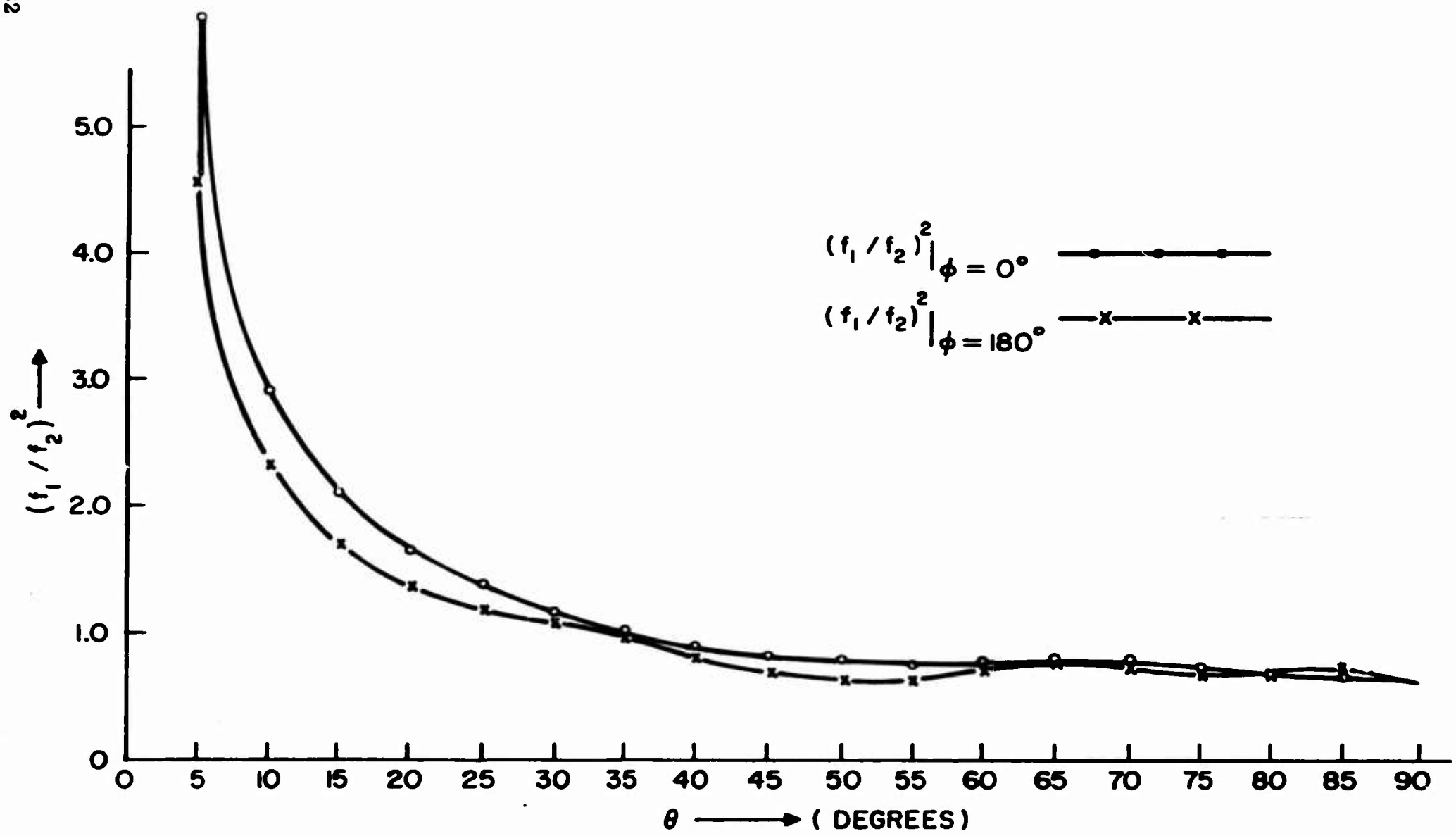

Figure 17. A comparison of $(f_1/f_2)^2|_{\varphi = 0^o}$ with $(f_1/f_2)^2|_{\varphi = 180^o}$ as a function of θ.

(2) f_1/f_2 is single valued for $0^o \leq \theta \leq 90^o$.

(3) The radiation modes are orthogonal.

(4) R_1 and R_2 are independent of φ.

The passive direction finder using the Archimedian spiral antenna generates information of low accuracy and is therefore of limited usefulness. Sufficient experimental information is not presently available to enable the prediction of possible improvement in accuracy.

7. REFERENCES

1. Kaiser, J. A., et al, "A Passive Automatic Direction Finder," Proc. IRE Ninth Annual East Coast Conference on Aerospace and Navigational Electronics, 3.2.3-1 to 3.2.3-4, Oct 1962.

2. Op. cit. page 3.2.3-4.

3. Cheo, B. R., "A Solution to the Equiangular Spiral Antenna Problem," Electronic Research Lab., University of California, Berkeley, Series No. 60, Issue No. 324, Nov 1960.

APPENDIX A

Comparison of true and computed values of φ (degrees); $\theta = 30^{o}$;

True Value	Deviation From True Value	True Value	Deviation From True Value
0	-5.8	180	+8.7
15	-4.9	195	+7.9
30	-2.2	210	+1.8
45	+1.1	225	-1.4
60	+4.4	240	-4.6
75	+2.5	255	-1.1
90	-0.4	270	-1.9
105	-4.8	285	+9.3
120	-0.9	300	+14.1
135	+2.5	315	+9.6
150	+7.0	330	+1.4
165	+8.4	345	+2.6

RMS error = 5.82^{o}

APPENDIX B

Least-square exponential curve approximation

Span the "signal space" by the three exponentials chosen in section 3. Think of these exponentials as existing on the finite interval $0 \leq \beta \leq 55^{o}$ and as zero outside the interval. $g(\alpha)$ is to approximate $\mathfrak{J}(\alpha)$ in the least-square sense by the proper choice of β's in equation (B1).

$$g(\alpha) = \beta_1 e^{k_1\alpha} + \beta_2 e^{k_2\alpha} + \beta_3 e^{k_3\alpha} \qquad \text{(B1)}$$

the β's may be found by solving the equations

$$\begin{pmatrix} a_1 \\ a_2 \\ a_3 \end{pmatrix} = \begin{pmatrix} a_{11} & a_{12} & a_{13} \\ a_{21} & a_{22} & a_{23} \\ a_{31} & a_{32} & a_{33} \end{pmatrix} \begin{pmatrix} \beta_1 \\ \beta_2 \\ \beta_3 \end{pmatrix}$$

or

$$a = G\,\beta, \quad \beta = G^{-1} a$$

where $a_i = \int_o^{55^{o}} \mathfrak{J}(\alpha)\, e^{k_i\alpha} d\alpha \qquad i = 1, 2, 3$

and $a_{ij} = \int_o^{55^{o}} e^{k_i\alpha} e^{k_j\alpha} d\alpha \qquad i = 1, 2, 3 \qquad j = 1, 2, 3$

when the a_{ij}'s are evaluated, G is found to be

$$G = \begin{pmatrix} 4.999 & 6.060 & 7.686 \\ 6.060 & 7.686 & 10.470 \\ 7.686 & 10.470 & 16.052 \end{pmatrix}$$

$$G^{-1} \begin{pmatrix} 23.79 & -29.04 & 7.547 \\ -29.04 & 36.60 & -9.971 \\ 7.547 & -9.971 & 2.952 \end{pmatrix}$$

$$a = \begin{pmatrix} 27.71 \\ 35.48 \\ 50.90 \end{pmatrix}$$

These equations are solved for β to get:

$$\beta_1 = 13.16,\ \beta_2 = -13.40,\ \beta_3 = 5.61$$

The components of $g(\alpha)$ are graphed in figure B1.

This approximation technique was derived from unpublished classroom lecture notes of Dr. W. H. Huggins, Johns Hopkins University.

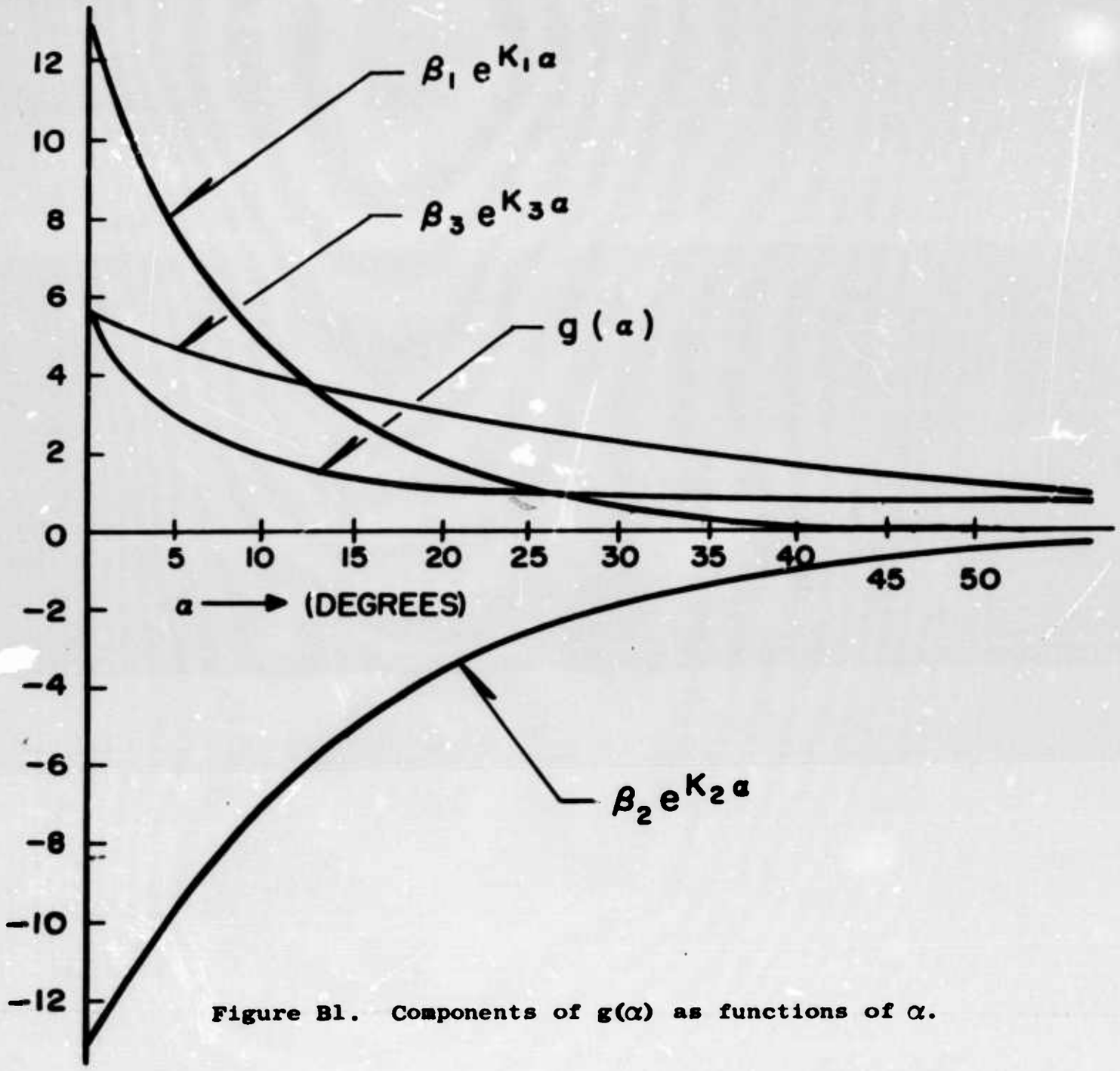

Figure B1. Components of $g(\alpha)$ as functions of α.